Available Online

J. Sci. Res. **16** (3), 783-801 (2024)

JOURNAL OF SCIENTIFIC RESEARCH

www.banglajol.info/index.php/JSR

Encapsulation of Biologically Potent Neurotransmitters into HP-β-CD Probed by Physicochemical Approach simultaneously Optimized by Computational Studies

F. Alam[1], S. B. Neogi[1,2], A. Das[1], N. Roy[1], A. Hossain[1], M. Kundu[1], L. Sarkar[3], M. N. Roy[1*]

[1]Department of Chemistry, University of North Bengal, Darjeeling-734013, India

[2]Department of Chemistry, Darjeeling Govt. College, Darjeeling-734101, India

[3]Department of Chemistry, Siliguri College, Darjeeling-734001, India

Received 8 November 2023, accepted in final revised form 14 February 2024

Abstract

The inclusion complexes of the neurotransmitters, namely (±) epinephrine hydrochloride, dopamine hydrochloride, and tyramine hydrochloride in an aqueous medium, were studied physicochemically and spectroscopically. These rendered systems of drug delivery with the potential to ensure delivery to desired targets. The stoichiometry of the 1:1 ratio of host-guest binding was established using Job plots. Conductimetric studies gained an understanding of inclusion as a process. Furthermore, ^{1}H NMR was used to characterize the inclusions, and the Benesi Hildebrand equation was applied to obtain the association constants. Thermodynamics, which are important in predicting the feasibility of any process, were in favor of inclusion as obtained by the evaluation of various thermodynamic parameters from Van't Hoff's equation.

Keywords: Neurotransmitter; Host-guest interaction; Inclusion complex; HP-β-CD.

doi: https://dx.doi.org/10.3329/jsr.v16i3.69752 J. Sci. Res. **16** (3), 783-801 (2024)

1. Introduction

The encapsulation of neurotransmitters of utmost biological importance is a key to interpreting and developing an understanding of formed molecular assemblies as an extension to find applications in potential drug delivery to the targeted sites of their action [1-3]. HP–β-CD owes its application to enabling pharmaceutical excipients by enhancing the solubility of a spectrum of drugs in the aqueous phase [4,5]. This is attributed to the toroidal configuration with innumerable hydroxyl groups at each of its ends, imparting it the ability to bind drug molecules with an even higher degree of hydrophobicity [6-8], thereby releasing it into biological systems with absolute ease while keeping its solubility in water intact. The polar exterior with hydroxyl groups is the key to aqueous solubility [2,3]. The factors stabilizing the binding inside the hydrophobic cavity are non-covalent Vander Waals forces, electrostatic forces, H-bonding, removal of energetically high water

*Corresponding author: mahendraroy2002@yahoo.co.in

bound to the cavity, and also the reduction in conformational strain post to the binding [6,7,9]. The formation of such supramolecular assemblies based on such forces was understood by interpreting results obtained through physicochemical studies like conductance measurement [6]. Controlled delivery of drugs based on HP-β CD as binders or carriers of drug molecules is a key to therapeutics [1]. It surpasses the lipophilic membranes of appreciable hydrophobicity [4,5] under the head of the inclusion complex to exert therapeutic action as desired by its target. This approach has potency in enhancing stability, bio-availability, and solubility in drug formulations [10-12]

The three chosen amines in their hydrochloride combinations are our molecular guests. Each of them belongs to the class of neurotransmitters occurring in biological systems that make significant contributions in conducting nervous impulses from one axon to the next dendritic tip of the neurons [6]. Dopamine is a neurotransmitter occurring in mammals that is necessary to ensure homeostasis [6,13,14]. Parkinsonism, a diseased condition, is again due to the deficiency in the occurrence of this biogenic amine and leads to improper neural and neuromotor functions [15]. Tyramine is yet another NT of interest and a Catecholamine releaser [16,17]. Epinephrine, the third amine taken, is also an NT and a hormone that chemically mediates impulses to the required organs [18,19]. It is an active medication for treating patients with cardiac arrest and other such disorders. [20-22]

Here, the formulations of drugs studied were dopamine, tyramine, and epinephrine in their hydrochloride combinations with HP- β-CD, respectively. The understanding of such supramolecular assemblies was gained using Job plots, conductance measurements, UV-VIS Spectroscopy, and ^{1}H NMR. The addition of a thermodynamic standpoint drew the parameters, the key to quantifying the complexation of each such amine with HP- β- CD. Thereby, the overall thermodynamics involved in the process are established [1].

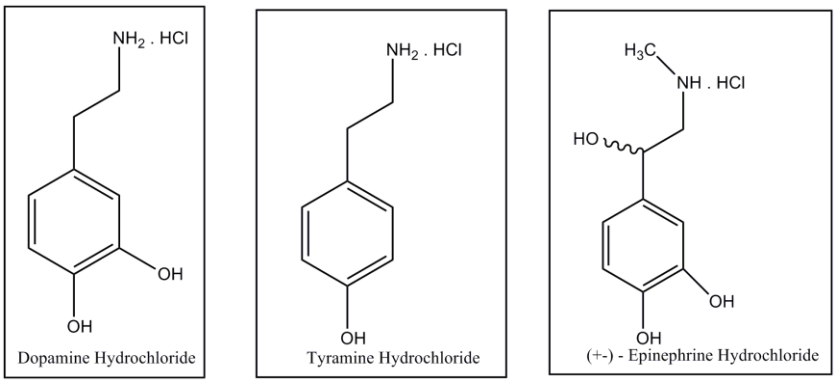

Scheme 1. Molecular structure of the neurotransmitters.

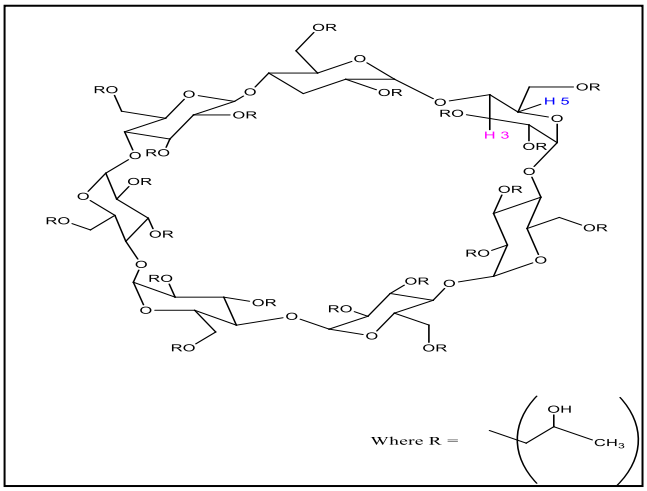

Scheme 2. 2D molecular structure of HP-β-CD.

2. Experimental Section

2.1. *Materials*

The procurement of dopamine hydrochloride (DH), tyramine hydrochloride (TH), and epinephrine hydrochloride (EH) were done from the German Company Sigma–Aldrich. These were used as obtained in hands. The associated purity of HP- β-CD, DH, TH, and EH were 99 %, 98 %, and 99 %, respectively.

2.2. *Apparatus and procedure*

Solubilities of the HP-β-CD and the biogenic amines (NT) selected were thoroughly checked with the triply distilled and degassed water before the experimental run. The water used had a specific conductance value of 1×10^{-6} S Cm^{-1}. In observation, all such NTs were soluble in every quantity of the aqueous solutions of the HP-β-CD. Stock solutions were prepared according to mass for each of the NT'S (weighing was done with the Mettler Toledo AG -285, and the uncertainty associated was 0.0003 g). At a temperature of 298.15K, a mass dilution was done to the prepared solutions. A handful of precautionary measures were followed during mixing to cut losses due to evaporation.

The spectrophotometer JASCO V-530 UV/VIS was used to record the UV–visible spectra. The uncertainty associated with its wavelength resolution was ± 2 nm. Constancy in measuring temperature was kept intact using a digital thermostat.Systronics 308 Conductivity Bridge and immersion conductivity cell CD-1 dip–type were used in the conductance studies. The conductivity cell was reported to have a cell constant value of 0.1 ± 0.001 cm^{-1}. HPLC grade water of Specific conductance 6.0 Sm^{-1} was used. Fresh 0.001 M aqueous KCl solutions were used to calibrate the conductivity cell before the experiment. An uncertainty of 3 % was found for the specific conductance values obtained.

Bruker ADVANCE 400 MHz was used to record the NMR spectra in D_2O. The δ values in ppm are the signal quotations. Other residuals were treated as due to internal standards, i.e. D_2O: 4.79 ppm. The chemical shifts are our data in hand.

3. Result and Discussion

3.1. *Stoichiometry of host-guest binding through job plots*

The UV-visible spectroscopy-based continuous variation method of Job was a key to understanding the stoichiometry of host-guest binding [6,23]. The plot of ΔA × R VS R generated the Job plots, here, ΔA denotes the absorbance difference values for the NT's while complexes and free of HP - β- CD denoted as R = [NT] / ([NT] + [CD]). Then, variation in mole fraction was undertaken for the NTs in the 0-1 range (Supporting information is held up with tables S1, S2, S3) [6,24]. The values for the absorbances were recorded at their respective λ_{max} for the experimental solutions, all recorded at a temperature of 298.15 K. At the maximum deviation, the value of R was evident in the stoichiometry of the inclusion complex (IC) (e.g., 1:1 complexes, 1:2 complexes, and 2:1 complexes, respectively, gave R values 0.5, 0.33 and 0.66. Our maxima were all found at R = 0.5 for all of the three plots. This obtained value of R established a stoichiometry of 1:1 binding for the host-guest.

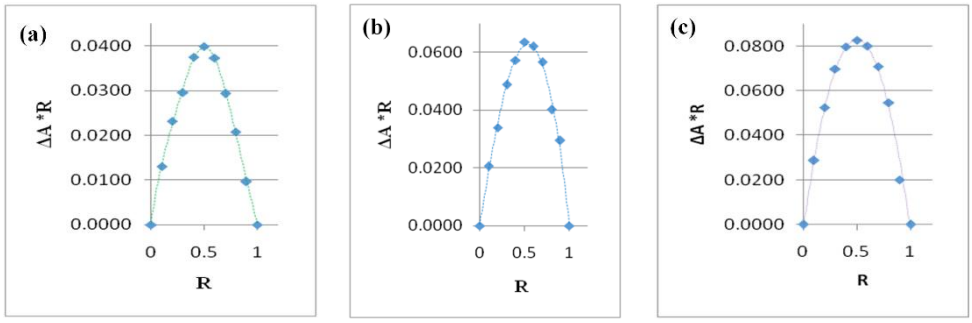

Fig. 1. Job plot of various neurotransmitter-HP-β-CD complexes at 298.15 K. (a) DH at λ_{max} = 280 nm, (b) TH at λ_{max} = 275 nm, and (c) EH at λ_{max} = 279 nm. R = [NT]/([NT] + [HP-β-CD]), ΔA = difference in absorbance of NTs with and without HP-β-CD.

3.2. Conductance *illustration of the inclusion and the stoichiometry involved*

The conductance measurements for the NTs' aqueous solutions were performed to determine if the ICs were produced with the addition of the host HP-β- CD to these solutions [25,26]. An appreciable value for the 'κ' was an illustration of the NTs as charged structures. Furthermore, the values for 'κ' were seen to exhibit a decreasing trend upon the addition of the host HP-β- CD, indicative of the binding of the guest NTs to the host. A break in each of these curves for conductance for a specific concentration of HP-β-CD indicated successful inclusion. The HP-β-CD concentration and the κ value corresponding to the

breaks in each of these curves are tabulated in Table (S4). This established that the breakpoint ratio of the [NT] / [HP-β- CD] is approximately 1:1 and thus follows to establish the host-guest ratio binding to be 1:1.

The breakpoint corresponds to the concentration with the maximum possible inclusion. The process upholds an equilibrium of the dynamic type involved, but the keynote is that the encapsulation or formation of assemblies is more ready for most molecules only at this breaking point (Host (conc) / Guest (conc)) = 1:1. The concentration of HP-β-CD exceeds that of NT beyond this breakpoint and is indicative of the equilibrium shifting towards the inclusion formation.

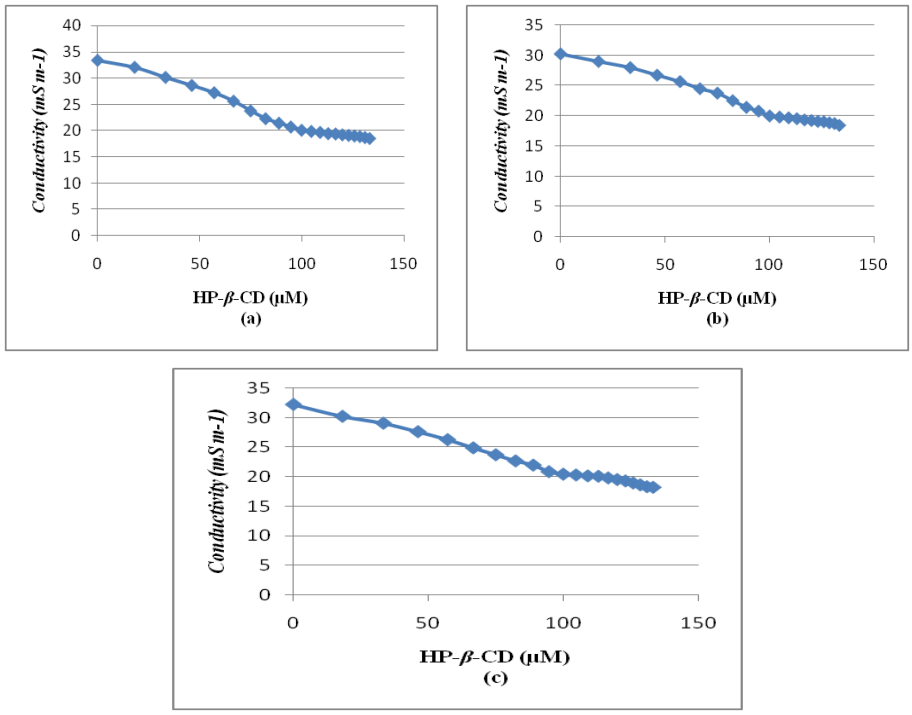

Fig. 2. Change in the conductivity of aqueous (a) DH solution, (b) TH solution, and (c) EH solution with the addition of HP-β-cyclodextrin at 298.15 K.

3.3. *^{1}H NMR studies*

The NMR study is key to interpreting the extent of inclusion of the guest molecule in the host [27,28]. For the taken NTs, the values of the H3 and H5 post-to inclusion explain the ease with which each inclusion of the guests occurs in the hydrophobic cavity of the HP-β-CD [29,30].

Table 1. Shifting of ^{1}H NMR values of NTs.

Drug	Position of the proton	Pure	IC.	Shift
Dopamine	H2	2.78–2.81 (2H, t, J = 7.2 Hz)	2.76-2.8 (2H, t, J = 7.2 Hz)	-0.019
	H1	3.13–3.16 (2H, t, J = 7.2 Hz)	3.10-3.13 (1H, dd, J = 8.0, 1.6 Hz)	-0.039
	Ar-H	6.76–6.77 (1H, d, J = 2 Hz),	6.72–6.73 (1H, d, J = 2 Hz),	-0.046
Epinephrine	H1	2.68 (3H, s)	2.67 (3H, s)	-0.013
	H4	4.81–4.84 (1H, t, J = 6.4 Hz)	4.78-4.81 (1H, t, J = 6.4 Hz)	-0.04
	Ar-H	6.85–6.87 (2H, m)	6.81-6.82 (2H, m)	-0.04
Tyramine	H2	2.82–2.86 (2H, t, J = 7.2 Hz)	2.82-2.86 (2H, t, J =7.2 Hz)	-0.007
	H1	3.14–3.17 (2H, t, J = 7.2 Hz)	3.11-3.15 (2H, t, J = 7.2 Hz)	-0.029
	H4	6.81–6.83 (2H, dd, J= 6.8, 2.0 Hz)	6.78-6.8 (2H, dd, J = 6.8, 2.0 Hz)	-0.02
	H3	7.12–7.14 (2H, d, J = 8.8 Hz)	7.10-7.13 (2H, d, J = 8.8 Hz)	-0.03

Table 2. Shifting of ^{1}H NMR values of HP-β-CD.

	Position of the proton of HP-β-CD	Pure HP-β-CD	IC	Shift
Dopamine	H3	3.69-3.82 (6H, m)	3.67-3.8 (6H, m)	-0.02
	H5	3.89-3.99 (6H, m)	3.87-3.97 (6H, m)	-0.02
Epinephrine	H3	3.69-3.82 (6H, m)	3.65-3.78 (6H, m)	-0.04
	H5	3.89-3.99 (6H, m)	3.85-3.95 (6H, m)	-0.04
Tyramine	H3	3.69-3.82 (6H, m)	3.69-3.82 (6H, m)	0.00
	H5	3.89-3.99 (6H, m)	3.88-3.98 (6H, m)	-0.01

The values of chemical shifts for H3 and H5 were recorded respectively as (0.00, -0.01) for tyramine, (-0.02, -0.02) for dopamine, and (-0.04, -0.04) for epinephrine. This indicates that the extent of inclusion is maximum for epinephrine, with the most negative values of the chemical shift for H3 and H5, followed by tyramine with intermediate negative values of the chemical shifts, further followed by the least negative value of the chemical shifts for the same in case of dopamine. Alternatively, the ease of inclusion with HP-β-CD decreases from epinephrine to dopamine to tyramine**.**

3.4. *Calculation of the association constants and thermodynamic parameters*

The UV-VIS Spectroscopy was used to evaluate the association constants (Ka) for the ICs of NTs with the HP-β-CD. This was obtained due to the change in values of the Δε, the molar extinction coefficient, of the NT+HP-β-CD complexes. This observation is attributed to the variation in polarity of the immediate vicinity of the Chromophores present in the neurotransmitters on the transition to the hydrophobic non-polar toroidal cavity from an entirely polar aqueous surrounding [31,32]. The determination of Ka was done by studying the change in ΔA, the absorption intensity of the DH (S5), TH (S6), and EH (S7) as HP-β-CD's concentration function. The Benesi-Hildebrand method was applied further to obtain the double reciprocal plots, as is the case for 1:1 host-guest ICs.

$$1/\Delta A = 1/\Delta\varepsilon\,[NT]\,Ka \times 1/[HP\text{-}\beta\text{-}CD] + 1/\Delta\varepsilon\,[NT]$$

The Intercept obtained for the double reciprocal plot was divided to obtain the values of Ka for the three inclusions [33].

A probe to the thermodynamic standpoint was delved to evaluate parameters of thermodynamic importance and extended to the inclusion as a process with the well-known Van't Hoff equation. It correlates thermodynamic parameters with Ka. Thus, known Ka parameters like ΔH°, ΔS°, and ΔG° were derivable from the equation stated below:

$$\ln Ka = - \Delta H°/ RT + \Delta S°/R$$

The equation shows linearity between ln Ka/2.303 and 1/T. The thermodynamic parameters stated above, along with ΔG°, are all derivable for the inclusions performed [34].

The study undertaken for the ΔH^0 and ΔS^0 are constant for the short range of temperature taken here. However, a Non-Linear approach is to be used while studying the same parameters for a wider range of temperatures. Direct calorimetric methods are associated with more accuracy concerning the ΔH^0, as these are dependent on equilibrium constants for the IC as a function of temperature [35].The Δε of the NTs was the determinant for the obtained Ka, which was the basis for the obtained thermodynamic parameters. This followed as a direct consequence of the changes near the chromophores in the NTs. Owing to the transition to an apolar cavity from a polar region. The solvent interactions are non-contributing to the obtained ΔH° and ΔS° and are only defined for the formed molecular complexes of interest.

A feasible process that is an inclusion formation was laid from the negative values of the ΔG°. The negative enthalpy (ΔH°) and negative entropy (ΔS°) indicate that the process of inclusion is an exothermic. It also establishes that the process is not entropy-driven. The above-mentioned observations are in favor of the association developed in the course of inclusion between the host-guest pair, thereby cutting down randomization and a drop in entropy,favoring inclusion on the whole. The mentioned entropy effect is more than overweighed by the larger negative values for the ΔH°, establishing overall favorable thermodynamics for inclusion formation.

The Table S8 for the order of –ΔG° and Ka is EH> DH> TH. The ease of getting included inside the non-polar cavity is in the same order as that stated above. This is an immediate result following the structures of the guest NTs with comparable hydrophobic moieties. However, a point of difference is the variable numbers of the polar –OH groups in each of them. With 2 –OH groups of phenolic nature and 1- OH group of alcoholic nature in EH, it forms a strongly associated inclusion by H-bond formation. Following EH with the strongest such inclusion among the three, DH and TH form less and least stronger associations on account of the possession of the two and only one –OH group in their structures, respectively.

3.5. *Preparation of 3D-structures of T.Y., D.O.P., EPI and HP-β-CD*

The three-dimensional structures of DH, TH, and EH were obtained from the PubChem website (http://pubchem.ncbi.nlm.nih.gov). HP-β-CD was constructed from β-CD by adding a hydroxypropyl group, and β-CD was taken from Cambridge Crystal Data Centre (CCDC) with a deposit number (CCDC ID: 762697) [36]. Before conducting the computational investigations, the missing hydrogen atoms and the charges of the atoms

were added to HP-β-CD as well as DH, TH, and EH structures, and the optimization was done with the DFT-B3LYP method using Gaussian 09 software [37].

3.6. *Molecular docking evaluation*

Molecular docking is a computer-based analysis that assists in determining the preferred binding mode of a guest with a host [38,39]. A well-established docking procedure for the PyRx host-guest system was employed. [40]. Before conducting docking, PDB files of DH, TH, EH, and HP-β-CD were transformed into PDBQT format, and the atomic coordinates were generated using PyRx software. For all three DH-HP-β-CD, TH-HP-β-CD, and EH-HP-β-CD complex, the center values of the grid box were set as center x= 8.4381, center_y= 24.3525 and center_z= 1.6111, and the values of dimension as size_x= 25, size_y = 25, and size_z = 25 for all three coordinates. The grid box size was taken around the binding cavity of HP-β-CD (receptor) to sufficiently allow the ligand to move without any constraint in the search space. Based on the docking score, the conformer with the lowest docked energy was selected [41], and for visualizations, Discovery Studio Visualizer, v21.1.0.20298, BIOVIA, was used [42].

3.7. *Molecular docking studies*

Molecular docking has been widely utilized to anticipate the binding orientation of a guest into the host pocket[43,44]. With the help of PyRx software, the docking has been done between NTs and HP-β-CD. The most favorable docked conformation of the Guest-HP-β-CD complex is shown in Fig 3. The negative binding energy (ΔG) with the lowest value associated with the docked conformation, which has maximum stability of TH-HP-β-CD, DH-HP-β-CD, and EH-HP-β-CD-complex was found to be -5.20 kcal/mol, -5.60 kcal/mol and -5.70 kcal/mol which is very close to the value collected from other studies, implicating that the binding energy obtained from docking is almost similar to the value obtained from other analysis. Docking results suggested that all three complexes and the guest molecules were completely incorporated in the hydrophobic cavity of HP-β-CD through the wider end. These interactions of guest molecules with HP-β-CD gathered from the docking study are aligned with the observations of ^{1}H NMR analysis also.

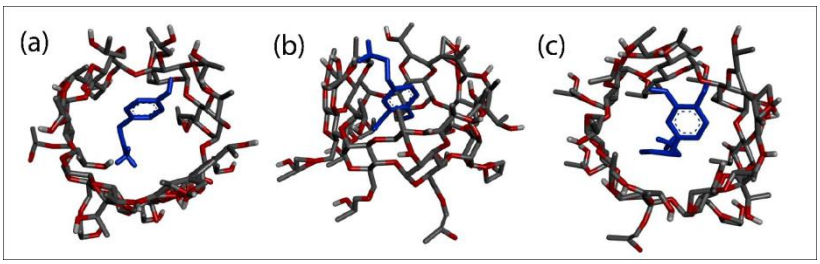

Fig. 3. 3D structural representation of optimized structures of (a) TH-HP-β-CD, (b) DH-HP-β-CD, (c) EH-HP-β-CD.

4. Conclusion

The exploration of ICs with NTs attempted to develop potential drug deliveries for applications in medicinal chemistry. The Jobs plot and conductance study established 1:1 inclusion. Furthermore, the association constants also indicated that the extent of inclusion is maximum for epinephrine, followed by dopamine, which tyramine again follows.

The thermodynamic parameters ΔH°, ΔS°, and ΔG° also indicated the same as those established before. The NMR study also provides evidence of the same fact. Additionally, the ΔG° obtained either from the molecular docking or association constant assumes values very close to each other. This also indicated that the extent of inclusion is maximum for the epinephrine and minimum for the tyramine. The result obtained is the same for all approaches.

References

1. S. Saha, M. Kundu, B. C. Saha, S. Barman, and M. N. Roy, Chem. Phys. Lett. **655-656**, 43 (2016). http://dx.doi.org/10.1016/j.cplett.2016.05.031
2. E. M. M. D. Valle, Process Biochem. **39**, 1033 (2004). http://dx.doi.org/10.1016/S0032-9592(03)00258-9
3. B. G. Mathapa and V. N. Paunov, Phys. Chem. Chem. Phys. **15**, 17903 (2013). https://doi.org/10.1039/C3CP52116H
4. G. Verma and P. A. Hassan, Phys. Chem. Chem. Phys. **15**, 17016 (2013). https://doi.org/10.1039/C3CP51207J
5. J. Ding, L. Chen, C. Xiao, L. Chen, X. Zhuang, and X. Chen, Chem. Commun. **50**, 11274 (2014). https://doi.org/10.1039/C4CC03153A
6. K. Roy, P. Bomzan, and M. Chandra Roy, J. Mol. Liq. **230**, ID 104 (2016) https://doi.org/10.1016/j.molliq.2016.12.104
7. M. V. Rekharsky and Y. Inoue, Chem. Rev. **98**, 1875 **(**1998),https://doi.org/10.1021/cr970015o
8. M. V. Rekharsky, R. N. Goldberg, F. P. Schwarz, Y. B. Tewari, P. D. Ross et al., J. Am. Chem. Soc.**117,** 8830 **(**1995) https://doi.org/10.1021/ja00139a017
9. S. Li and W. C. Purdy, Chem. Rev. **92,** 1457 **(**1992) https://doi.org/10.1021/cr00014a009
10. K. A. Connors, Chem. Rev. **97**, 1325 (1997) . https://doi.org/10.1021/cr960371r
11. Y. Kang, K. Guo, B. -J. Li, and S. Zhang, Chem. Commun. **50**, 11083 (2014). https://doi.org/10.1039/C4CC03131H
12. S. M. N. Simoes, A. R. Rico, A. Concheiro, and C. A. Lorenzo, Chem. Commun. **51**, 6275 (2015). https://doi.org/10.1039/C4CC10388B
13. G. Di Giovanni, V. Di Matteo, and E. Esposito, Serotonin-dopamine Interaction: Experimental Evidence and Therapeutic Relevance (Elsevier, Amsterdam, 2008). https://doi.org/10.1016/S0079-6123(08)00903-5
14. K. A. Conway, J. C. Rochet, R. M. Bieganski, and P. T. Lansbury Jr, Science **294**, 1346 (2001). https://doi.org/10.1126/science.1063522
15. H. Wood, Nat. Rev. Neurol. **10**, 305, (2014). https://doi.org/10.1098/rstb.2013.0507
16. G. D. Andrea, G.P. Nordera, F. Perini, G. Allais, and F. Granella, Neurol. Sci. **28**, S94 (2007). https://doi.org/10.1007/s10072-007-0758-4
17. K. Engelman and A. Sjoerdsma. JAMA **189**, 81 (1964). https://doi.org/10.1001/jama.1964.03070020009002
18. O. B. Halbach, R. Dermietzel, Neurotransmitters and Neuromodulators: in Handbook of Receptors and Biological Effects, 2nd Edition (Wiley, 2006).
19. T. Miyashita and C. Williams, C. Neurobiol. Learn. Memory **85**, 116 (2006). https://doi.org/10.1016/j.nlm.2005.08.013

20. N. L. Caroline, B. Elling, M. Smith, Nancy Caroline's Emergency Care in the Streets, ed. Jones et al., 7th Edition (2013).
21. R.A. Rhoades, D.R. Bell, Medical Physiology: Principles for Clinical Medicine, 7th Edition (Lippincott Williams & Wilkins, 2013).
22. Nielsen, Niklas, K. Sunde, J. Hovdenes, R. R. Riker, S. Rubertsson, P. Stammet, F. Nilsson, and H. Friberg. Crit. Care Med. **39**, 57 (2011). https://doi.org/10.1097/CCM.0b013e3181fa4301
23. P. Job, Ann. Chim. **9**, 113 (1928).
24. J. S. Renny, L. L. Tomasevich, E. H. Tallmadge, and D. B. Collum, Angew. Chem. Int. Ed. **52**, 11998 (2013). https://doi.org/10.1002/anie.201304157
25. A. Apelblat, E. Manzurola, Z. Orekhova, J. Solut. Chem. **36**, 891 (2007). https://doi.org/10.1007/s10953-007-9156-z
26. T. Qian, C. Yu, S. Wu, and J. Shen, Colloids Surf. B **112**, 310 (2013). https://doi.org/10.1016/j.colsurfb.2013.08.005
27. G. Fronza, A. Mele, E. Redenti, and P. Ventura, J. Org. Chem. **61**, 909 (1996). https://doi.org/10.1021/jo951410
28. J. Li, M. Zhang, J. Chao, and S.Shuang, Spectrochim. Acta-A: Mol. Biomol. **73**, 752 (2009) https://doi.org/10.1016/j.saa.2009.03.025
29. V. Sindelar, M. A. Cejas, F. M. Raymo, W. Chen, S. E. Parker, and A. E. Kaifer, Chem. Eur. J. **11**, 7054 (2005). https://doi.org/10.1002/chem.200500917
30. T. Wang, M. D. Wang, C. Ding, and J. Fu, Chem. Commun. **50**, 12469 (2014). http://xlink.rsc.org/?DOI=c4cc05677a
31. J. V. Caso, L. Russo, M. Palmieri, G. Malgieri, S. Galdiero et al., Amino Acids, **47**, 2215(2015). https://doi.org/10.1007/s00726-015-2003-4
32. H.A. Benesi and J.H. Hildebrand, J. Chem. Soc. **71**, 2703 (1949). https://doi.org/10.1021/ja01176a030
33. Y. Dotsikas, E. Kontopanou, C. Allagiannis, and Y. L. Loukas, J. Pharm. Biomed. Anal. **23**, 997 (2000). https://doi.org/10.1016/S0731-7085(00)00392-7
34. Y. He and X. Shen, J. Photochem. Photobiol. A: Chem. **197**, 253 (2008). https://doi.org/10.1016/j.jphotochem.2008.01.001
35. R. D. Lisi, G. Lazzara, and S. Milioto, Phys. Chem. Chem. Phys. **13**, 12571 (2011). https://doi.org/10.1039/C1CP20737G
36. A. I. Ramos, T. M. Braga, P. Silva, J. A. Fernandes, P. Ribeiro-Claroet al., Cryst. Eng. Comm, **15**, 2822 (2013). https://doi.org/10.1039/C3CE26414A
37. M. J. Frisch, G. W. Trucks, H. B. Schlegel, G. E. Scuseria, M. A. Robb et al., Gaussian 09, Revision D.01 (Gaussian, Inc., Wallingford CT, 2016).
38. N. Roy, P. Bomzan, B. Ghosh, and M. N. Roy, New J. Chem. **47**, 1045 (2023). https://doi.org/10.1039/D2NJ05291A
39. S. Paul, J. Hossen, and T. K. Pal, J. Sci. Res. **14**, 309 (2022). https://doi.org/10.3329/jsr.v14i1.53713
40. S. Dallakyan and A. J. Olson, Chem. Biol. **243** (2015).
41. P. Rajkumar, S. Sundari,S. Selvaraj, A. Natarajan, R. Suganya et al., J. Sci. Res. **14**, 671 (2022).https://doi.org/10.3329/jsr.v14i2.56648
42. M. A. F. Yahaya, A. R. A. Bakar, J. Stanslas, N. Nordin, M. Zainol, and M. Z. Mehat, BMC Biotechnol. **21**, 38 (2021). https://doi.org/10.1186/s12896-021-00697-4
43. P. Rajkumar, S. Selvaraj, R. Suganya, D. Velmurugan, S. Gunasekaran, and S.Kumaresan, Chem. Data Collect. **15-16**, 10 (2018). https://doi.org/10.1016/j.cdc.2018.03.003
44. K. Thirunavukkarasu, P. Rajkumar, S. Selvaraj, R. Suganya, M. Kesavan et al., J. Mol. Struc. **1173**, 307 (2018). https://doi.org/10.1016/j.molstruc.2018.07.003

Supporting data

Conductivity

Table S4 shows the concentration and corresponding conductivity at which maximum inclusion took place (breakpoint at the curve) calculated by solving the equations of two intercepting straight lines. For example, consider the dopamine hydrochloride and HP-β-cyclodextrin system.

$$\kappa = -0.141\ c + 34.45 \quad (1)$$

$$\kappa = -0.044\ c + 24.49 \quad (2)$$

Solving equation (1) and (2),

$\kappa = 29\ mS \bullet m^{-1}$ and $c = 102.68\ \mu M$

Table S1. Job plot is mapped out by UV-Vis spectroscopy for aqueous dopamine hydrochloride(DH)-HP-*β*-CD solution at 298.15K[a].

DH (mL)	*HP-β*-CD (mL)	DH (μM)	*HP-β*-CD (μM)	[D]/([D]+[HP-*β*-CD])	Absorbance (A)	ΔA	ΔA×[D]/([D]+[HP-*β*-CD])
0.0	1.0	0	100	0.0	0.0000	0.2301	0.0000
0.1	0.9	10	90	0.1	0.02422	0.2058	0.0206
0.2	0.8	20	80	0.2	0.06037	0.1697	0.0339
0.3	0.7	30	70	0.3	0.06758	0.1625	0.0487
0.4	0.6	40	60	0.4	0.08711	0.1430	0.0572
0.5	0.5	50	50	0.5	0.10291	0.1272	0.0636
0.6	0.4	60	40	0.6	0.12663	0.1034	0.0621
0.7	0.3	70	30	0.7	0.14924	0.0808	0.0566
0.8	0.2	80	20	0.8	0.17994	0.0501	0.0401
0.9	0.1	90	10	0.9	0.19734	0.0327	0.0294
1.0	0.0	100	0	1.0	0.23006	0.0000	0.0000

[a]Standard ambiguity in temperature (T) = 0.01 K.

Table S2. Job plot is mapped out by UV-Vis spectroscopy for aqueous tyramine hydrochloride (TH)-HP-*β*-CD solution at 298.15K[a]

TH (mL)	*HP-β*-CD (mL)	TH (μM)	*HP-β*-CD (μM)	[T]/([T]+[HP-*β*-CD])	Absorbance (A)	ΔA	ΔA×[T]/([T]+[HP-*β*-CD])
0	3	0	100	0.0	0.0000	0.2008	0.0000
0.3	2.7	10	90	0.1	0.06993	0.1309	0.0131
0.6	2.4	20	80	0.2	0.08477	0.1161	0.0232
0.9	2.1	30	70	0.3	0.1021	0.0987	0.0296
1.2	1.8	40	60	0.4	0.10706	0.0938	0.0375
1.5	1.5	50	50	0.5	0.12104	0.0798	0.0399
1.8	1.2	60	40	0.6	0.138571	0.0623	0.0374
2.1	0.9	70	30	0.7	0.158884	0.0419	0.0294
2.4	0.6	80	20	0.8	0.1749	0.0259	0.0207
2.7	0.3	90	10	0.9	0.190092	0.0107	0.0097
3	0	100	0	1.0	0.20083	0.0000	0.0000

[a]Standard ambiguities in temperature (T) = 0.01 K.

Table S3. Job plot is mapped out by UV-Vis spectroscopy for aqueous (±)-epinephrine hydrochloride (EH)-HP--*β*-CD solution at 298.15K[a]

EH (mL)	*HP-β*-CD (mL)	EH (μM)	*HP-β*-CD (μM)	[E]/([E]+[HP-*β*-CD])	Absorbance (A)	ΔA	ΔA×[E]/([E]+[HP-*β*-CD])
0	3	0	100	0	0.0000	0.3523	0.0000
0.3	2.7	10	90	0.1	0.065253	0.2871	0.0287
0.6	2.4	20	80	0.2	0.089853	0.2625	0.0525
0.9	2.1	30	70	0.3	0.119843	0.2325	0.0697
1.2	1.8	40	60	0.4	0.153012	0.1993	0.0797
1.5	1.5	50	50	0.5	0.187284	0.1651	0.0825
1.8	1.2	60	40	0.6	0.218915	0.1334	0.0801
2.1	0.9	70	30	0.7	0.251276	0.1011	0.0707
2.4	0.6	80	20	0.8	0.284139	0.0682	0.0546
2.7	0.3	90	10	0.9	0.329909	0.0224	0.0202
3	0	100	0	1	0.352339	0.0000	0.0000

[a]Standard ambiguities in temperature (T) = 0.01 K.

Table S4. Conductivity results of aqueous dopamine hydrochloride (DH)-HP-*β*-CD, tyramine hydrochloride (TH)-HP-*β*-CD and (±)-epinephrine hydrochloride (EH)-HP-*β*-CD solution (concentration of stock solution of neurotransmitters =200X10^{-6}M, concentration of stock solution of HP-*β*-CD = 200X 10^{-6} M) at 298.15K[a]

Volm of HP-*β*-CD(mL)	Total vol (mL)	Conc of HP-*β*-CD (μM)0.000	Conc of Neurotranmitters(μM)	Conductivity of DH. (mS cm^{-1})	Conductuvity of T.H. (mS cm^{-1})	Conductuvity of E.H. (mS cm^{-1})
0	10	0.000	200	33.37	30.26	32.2
1	11	18.18	181.82	32.05	29.01	30.2
2	12	33.33	166.67	30.14	28	29.04
3	13	46.15	153.85	28.61	26.75	27.61
4	14	57.14	142.86	27.22	25.68	26.28
5	15	66.67	133.33	25.62	24.51	24.89
6	16	75.00	125.00	23.77	23.78	23.72
7	17	82.35	117.65	22.29	22.54	22.69
8	18	88.89	111.11	21.44	21.44	21.98
9	19	94.74	105.26	20.72	20.81	20.87
10	20	100.00	100.00	20.1	20.01	20.45
11	21	104.76	95.24	19.87	19.83	20.32
12	22	109.09	90.91	19.69	19.71	20.16
13	23	113.04	86.96	19.45	19.56	20.1
14	24	116.67	83.33	19.39	19.36	19.82
15	25	120.00	80.00	19.22	19.26	19.55
16	26	123.08	76.93	19.11	19.11	19.32
17	27	125.93	74.074	19.01	19.05	18.96
18	28	128.57	71.43	18.89	18.88	18.66
19	29	131.03	68.97	18.72	18.77	18.34
20	30	133.33	66.67	18.53	18.46	18.24

[a]Standard ambiguities in temperature (T) = 0.01 K.

Table S5. Benesi-Hildebrand double reciprocal plot is mapped out by UV-Vis spectroscopy for aqueous dopamine hydrochloride (DH)-HP-*β*-CD solution [A_0 = 0.0304].

Temp /K[a]	[DH] /μM	[HP-*β*-CD] /μM	A	ΔA	1/[HP-*β*-CD] /M^{-1}	1/ΔA	Intercept	Slope	K_a /M^{-1}
	50	30	0.04264	0.01224	33333	81.69935			
	50	40	0.04621	0.01581	25000	63.25111			
293.15	50	50	0.05102	0.02062	20000	48.49661	2.997	0.002	1498
	50	60	0.05314	0.02274	16666	43.97537			
	50	70	0.05792	0.02752	14285	36.33721			
	50	30	0.04195	0.01155	33333	86.58009			
	50	40	0.04541	0.01501	25000	66.62225			
298.15	50	50	0.05009	0.01969	20000	50.7872	2.65	0.002	1325
	50	60	0.05212	0.02172	16667	46.04052			
	50	70	0.05633	0.02593	14286	38.56537			
	50	30	0.04043	0.01003	33333	99.7009			
	50	40	0.04377	0.01337	25000	74.79432			
303.15	50	50	0.0482	0.0178	20000	56.17978	2.298	0.002	1149
	50	60	0.05033	0.01993	16666	50.17561			
	50	70	0.05192	0.02152	14285	46.4684			

[a]Standard ambiguities in temperature (T) = 0.01 K

Table S6. Benesi-Hildebrand double reciprocal plot is mapped out by UV-Vis spectroscopy for aqueous tyramine hydrochloride (TH)-HP-*β*-CD solution [A_0 = 0.09195].

Temp /K[a]	[T.H.] /μM	[HP-*β*-CD] /μM	A	ΔA	1/[HP-*β*-CD] /M^{-1}	1/ΔA	Intercept	Slope	K_a /M^{-1}
	50	30	0.09924	0.00729	33333	137.1742			
	50	40	0.10111	0.0092	25000	108.6957			
293.15	50	50	0.10331	0.01136	20000	88.02817	5.044	0.004	1261
	50	60	0.10606	0.01411	16667	70.87172			
	50	70	0.10839	0.01644	14286	60.82725			
	50	30	0.09808	0.00613	33333	163.1321			
	50	40	0.09979	0.00784	25000	127.551			
298.15	50	50	0.10184	0.00989	20000	101.1122	4.476	0.004	1119
	50	60	0.10399	0.01204	16667	83.05648			
	50	70	0.10567	0.01372	14286	72.8863			
	50	30	0.09733	0.00538	33333	185.8736			
	50	40	0.09878	0.00683	25000	146.4129			
303.15	50	50	0.10008	0.00813	20000	123.0012	4.902	0.005	980
	50	60	0.10274	0.0108	16667	92.59259			
	50	70	0.10426	0.0123	14286	81.30081			

[a]Standard ambiguities in temperature (T) = 0.01 K

Table S7. Benesi-Hildebrand double reciprocal plot is mapped out by UV-Vis spectroscopy for aqueous (±)-epinephrine hydrochloride(EH)-HP-*β*-CD solution [A_0 = 0.10594].

Temp /K[a]	[EH] /μM	[HP-*β*-CD] /μM	A	ΔA	1/[HP-*β*-CD] /M^{-1}	1/ΔA	Intercept	Slope	K_a /M^{-1}
	50	30	0.11328	0.00734	33333	136.2398			
293.15	50	40	0.11613	0.01019	25000	98.13543	4.74	0.003	1580
	50	50	0.11803	0.01209	20000	82.71299			

	50	60	0.12037	0.01443	16667	69.30007			
	50	70	0.12212	0.01618	14286	61.80852			
	50	30	0.11219	0.00625	33333	160.0000			
	50	40	0.11415	0.00821	25000	121.8027			
298.15	50	50	0.11599	0.01005	20000	99.50249	5.528	0.004	1382
	50	60	0.11795	0.01201	16667	83.26395			
	50	70	0.12005	0.01411	14286	70.87172			
	50	30	0.11102	0.00508	33333	196.8504			
	50	40	0.11301	0.00707	25000	141.4427			
303.15	50	50	0.11477	0.00883	20000	113.2503	6.025	0.005	1205
	50	60	0.11599	0.01005	16667	99.50249			
	50	70	0.11688	0.01094	14286	91.40768			

[a]Standard ambiguities in temperature (T) = 0.01 K

Table S8. Van't Hoff equation for calculating thermodynamic parameters ΔH^o, ΔS^o, and ΔG^o (298.15 K) of different neurotransmitter-HP-*β*-cyclodextrin inclusion complexes

	Temp /K[a]	K_a /M^{-1}	1/T	lnK_a	Intercept	Slope	ΔH^o /kJ mol^{-1}	ΔS^o /J mol^{-1} K^{-1}	ΔG^o /kJ mol^{-1}
	293.15	1498	0.003411	3.17494					
DH	298.15	1325	0.003354	3.12165	-0.313	1023	-8.50	-2.60	-7.73
	303.15	1149	0.003299	3.05977					
	293.15	1261	0.003411	3.10016					
TH	298.15	1119	0.003354	3.04828	-0.215	972.4	-8.08	-1.78	-7.55
	303.15	980	0.003299	2.99068					
	293.15	1580	0.003411	3.19808					
EH	298.15	1382	0.003354	3.13994	-0.367	1045	-8.68	-3.05	-7.78
	303.15	1205	0.003299	3.08043					

[a]Standard ambiguities in temperature (T) = 0.01 K

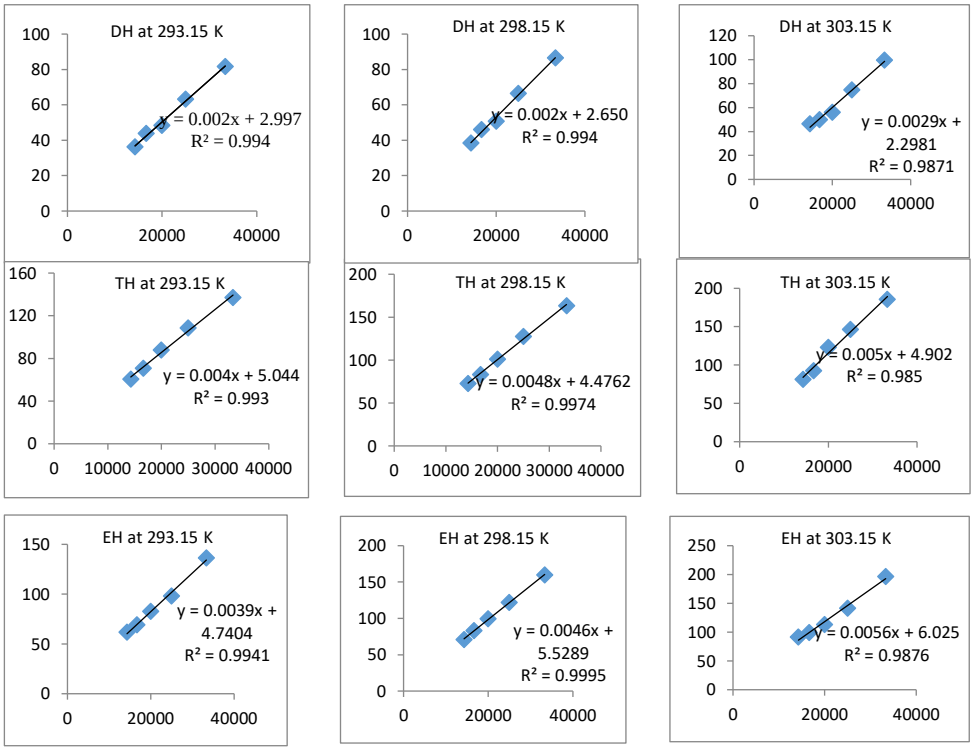

Fig. S1. Benesi-Hildebrand double reciprocal plot for the effect of HP-*β*-CD on the absorbance of DH (280 nm), TH (275 nm), and EH (279 nm) at different temperatures (X-axis = 1/[HP-*β*-CD] and Y axis = 1/ΔA).

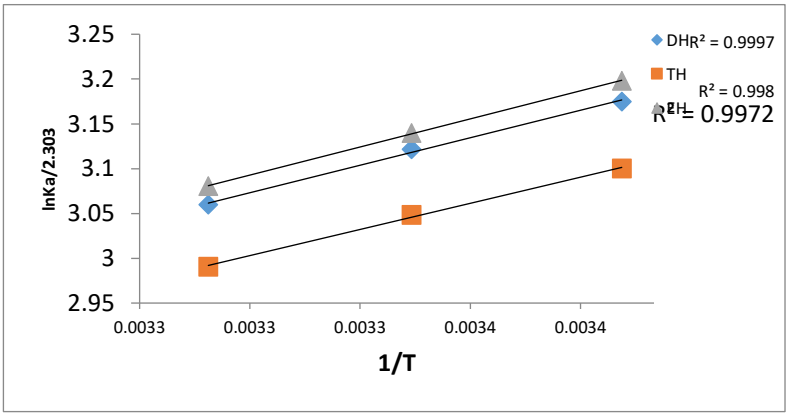

Fig. S2. The linear relationship of $\ln K_a/2.303$ vs. 1/T for the interaction between EH (▲), TH (■), and DH (◊) with HP- *β*-CD.

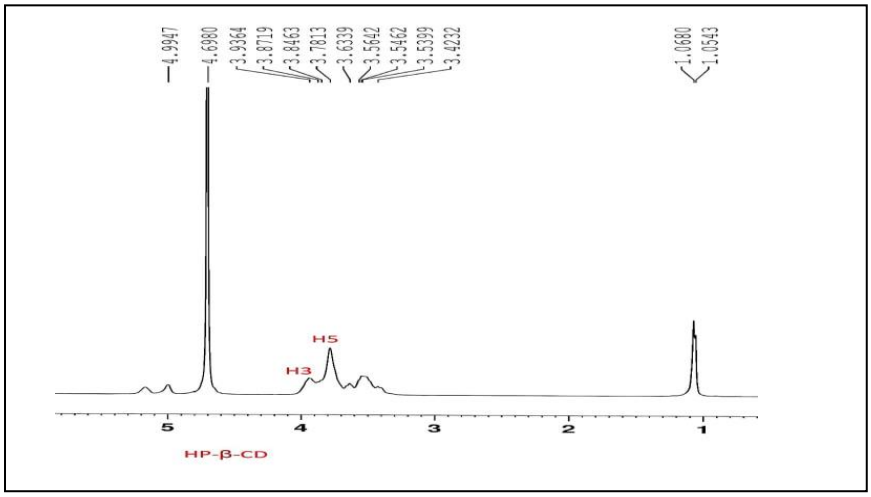

Fig. S3. [1]H NMR spectrum of HP-β-CD.

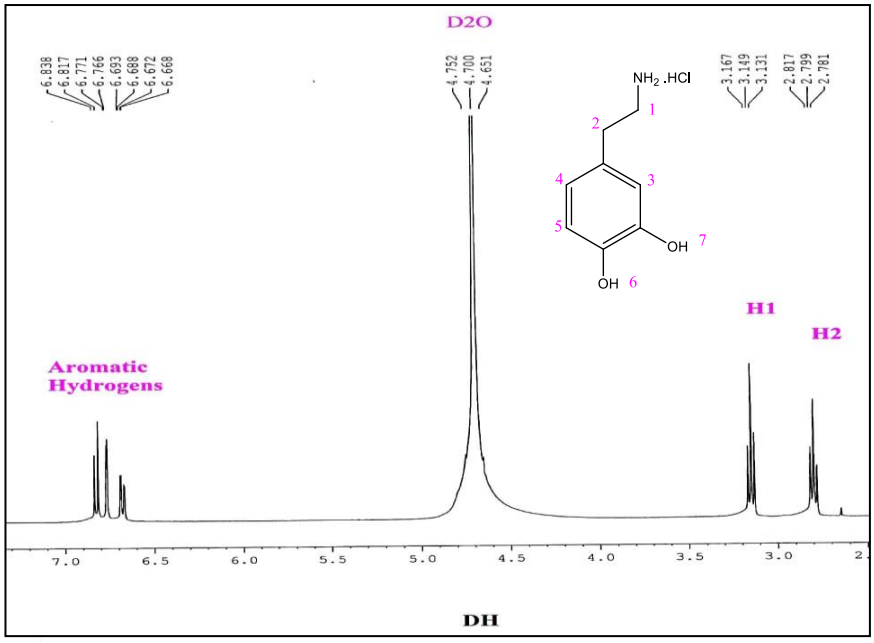

Fig. S4. [1]H NMR spectrum of dopamine hydrochloride (DH).

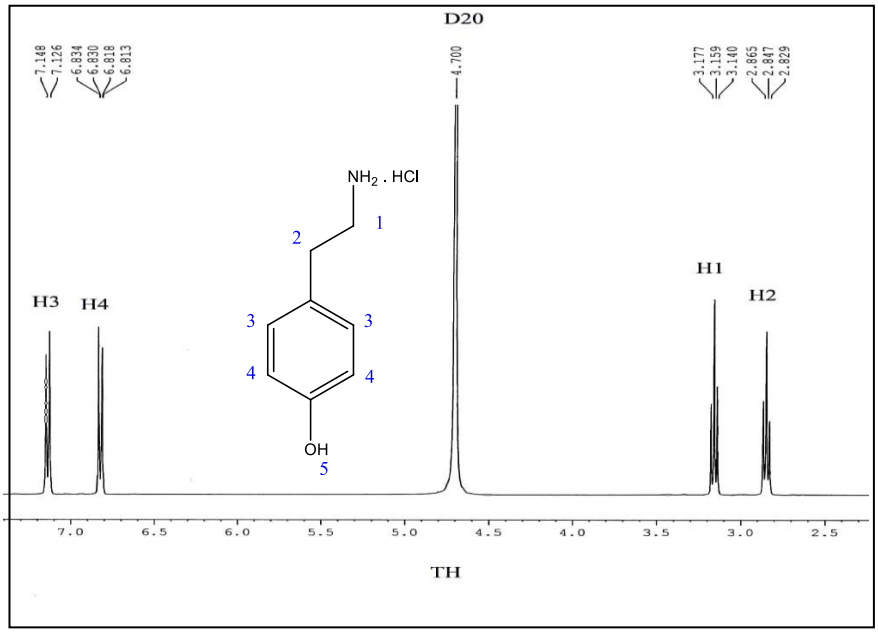

Fig. S5. ^{1}H NMR spectrum of tyramine hydrochloride (TH).

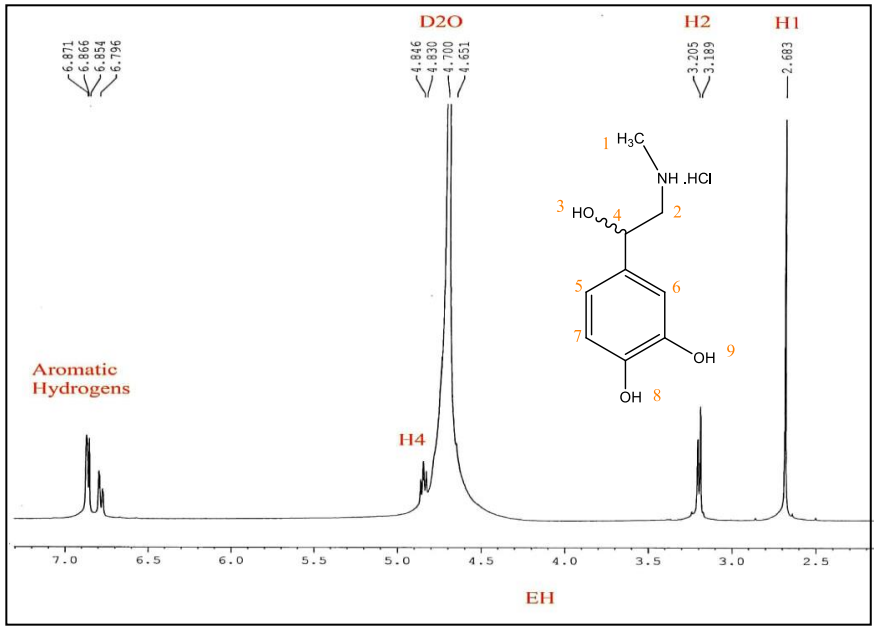

Fig. S6. ^{1}H NMR spectrum of epinephrine hydrochloride (EH).

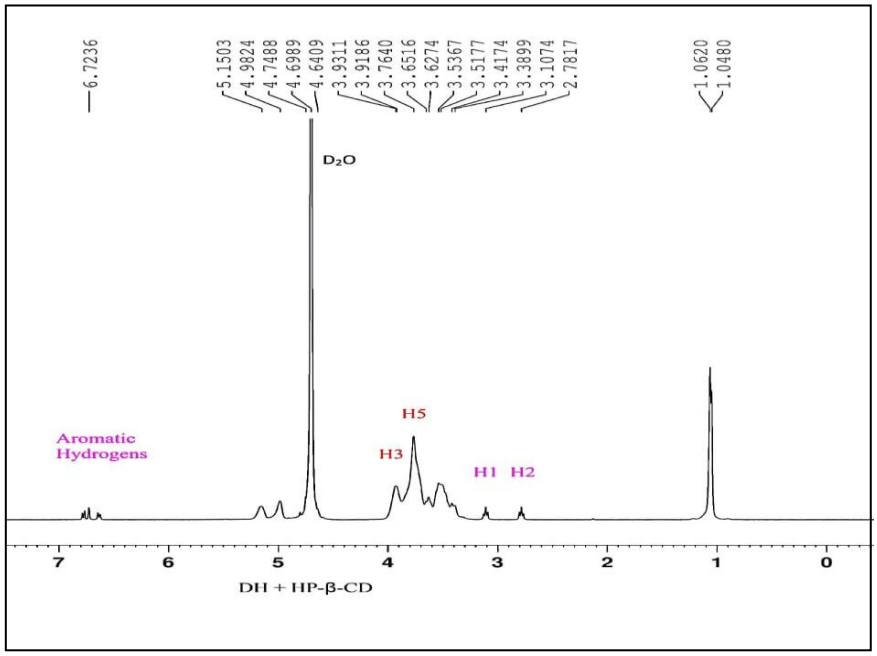

Fig. S7. ^{1}H NMR spectrum of DH + HP-β-CD.

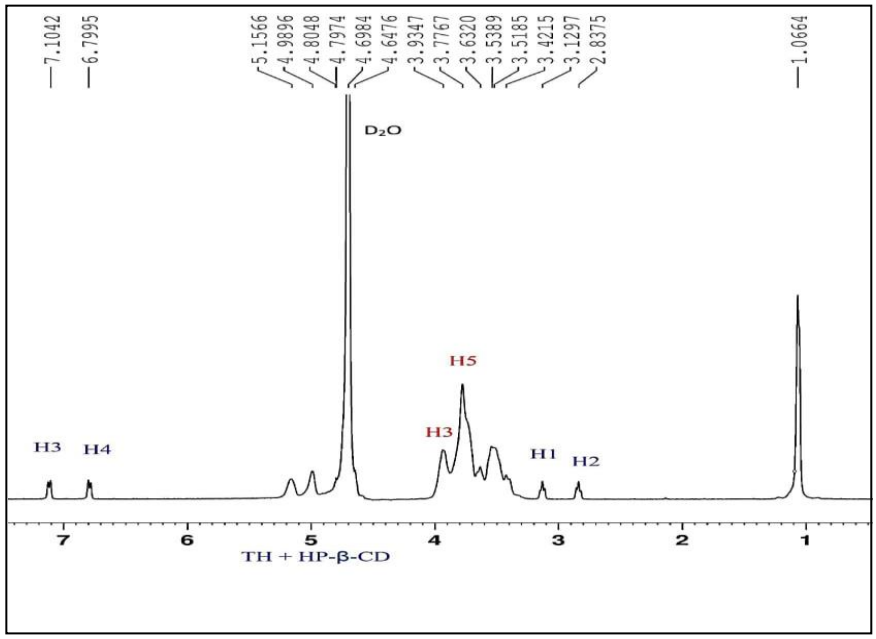

Fig. S8. ^{1}H NMR spectrum of TH+HP-β-CD.

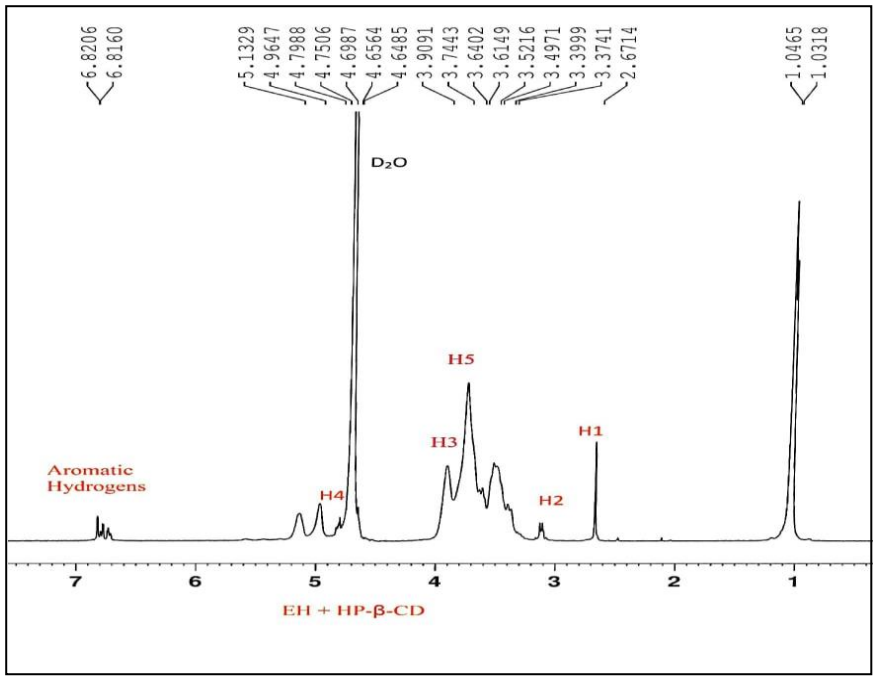

Fig. S9. ^{1}H NMR spectrum of EH+HP-β-CD.